

Moveout approximations for P- and SV-waves in transversely isotropic media with vertical axis of symmetry

Véronique Farra ¹ and Ivan Pšenčík ²

¹Institut de Physique du Globe de Paris, Sorbonne Paris Cité, Université Paris Diderot, UMR 7154 CNRS, F-75005 Paris, France. E-mail: farra@ipgp.fr

²Institute of Geophysics, Acad. Sci. of CR, Boční II, 141 31 Praha 4, Czech Republic. E-mail: ip@ig.cas.cz.

SUMMARY

We propose alternative expressions for the P- and SV-wave moveout formulae in VTI media based on the weak-anisotropy approximation. Our moveout formulae represent expansions with respect to small parameters, which are related to deviations of anisotropy from isotropy. First-order P-wave formulae depend on four parameters, two-way zero-offset traveltimes T_0 related to the vertical velocity α_0 , the depth H of the single horizontal reflector and two weak-anisotropy (WA) parameters ϵ_W and δ_W . The first-order SV-wave formulae depend on three parameters, again on T_0 now related to the SV-wave vertical velocity β_0 , depth H and the WA version of parameter σ . The second-order formulae are slightly more complicated. Both P- and SV-wave formulae depend on an additional parameter r , the ratio of the SV- and P-wave velocities. The SV-wave formula depends, in addition, on the WA parameter ϵ_W . Since the dependence of the moveout formulae on r is very weak, r can be specified as a typical SV- to P-wave velocity ratio and the number of parameters necessary to specify the second-order formulae is four for both waves. The formulae are relatively simple, highly accurate around zero offset and yield exact long-offset asymptote. Their accuracy at intermediate offsets depends on deviations of ray- and phase-velocity directions. The proposed formulae are also applicable in cases when the reflected ray is situated in a plane of symmetry of an orthorhombic medium, whose another symmetry plane is horizontal. This also includes any HTI medium with axis of symmetry in the plane containing the reflected ray.

1 INTRODUCTION

Reflection traveltimes (moveout) approximations find applications in several branches of processing of reflection data. There is quite an extensive literature devoted to these approximations in anisotropic media. For recent examples devoted to VTI (transverse isotropy with vertical axis of symmetry) media, see, e.g., Aleixo and Schleicher (2010),

Seismic Waves in Complex 3-D Structures, Report 23, Charles University, Faculty of Mathematics and Physics, Department of Geophysics, Praha 2013, pp. 81–103

Stovas (2010), or most recently Golikov and Stovas (2012). Many additional references can be found in these publications. For further references see Tsvankin (2001) or, e.g., Fomel and Stovas (2010). In most cases, the approximations are based on the Taylor expansion of the square of reflection traveltime T in terms of the square of the source-receiver offset x . If only the first and second terms of the expansion are kept, we speak about normal (hyperbolic) moveout, broadly used in reflection data processing in isotropic media. If the medium is anisotropic, the approximation based on the two terms becomes very inaccurate, especially for increasing offset. In fact, the moveout is generally non-hyperbolic in anisotropic media (if we do not consider elliptical anisotropy). In order to accommodate anisotropy, many researchers consider the next term in the Taylor expansion (Tsvankin, 2001) or use various multiparametric approximations based partially on physics and partially on intuition. A list of many such approximations for VTI media with illustrations of their accuracy can be found, for example, in Fowler (2003) or Aleixo and Schleicher (2010), see also Golikov and Stovas (2012). Quite accurate, but also quite complicated, formulae for homogeneous VTI media were proposed recently by Stovas (2010).

In this paper, we propose alternative reflection traveltime formulae for homogeneous VTI media, based on the weak-anisotropy (WA) approximation. Rather than expanding T^2 into a Taylor series in terms of x^2 , we expand T^2 in terms of the WA parameters, which characterize the deviation of anisotropy from isotropy. Our first-order formulae are specified by four parameters for P-waves: the two-way zero-offset traveltime T_0 , related to the vertical velocity α_0 , the depth H of the single horizontal reflector and two weak anisotropy (WA) parameters, linearized versions of Thomsen's (1986) parameters. In case of SV-waves, the first-order formulae are specified by three parameters: the two-way zero-offset traveltime T_0 , related to the vertical velocity β_0 , the depth H of the reflector and one WA parameter. In case of the second-order formulae, the WA parameter ϵ_W must additionally be considered in case of the SV-wave and an additional parameter r , the ratio of SV- to P-wave vertical velocity, must be considered for both waves. Because of the weak dependence of the moveout formulae on r , r can be specified as a typical SV- to P-wave velocity ratio and the number of parameters specifying the second-order P-wave moveout formula remains the same as in the first-order case and increases by one in the SV-wave case. If we do not take into account the depth H of the reflector, the proposed formulae for a P wave and the second-order formula for an SV-wave require the same number of parameters as the shifted hyperbola approximation (Malovichko, 1978, and his followers), by one parameter less than the rational approximation and by two parameters less than the generalized moveout formula, see Stovas (2010). The first-order SV-wave formulae require one parameter less. Note that some of the parameters are directly the WA parameters characterizing the structure or parameters related to them. The proposed formulae are relatively simple, for example, they do not contain square roots. Their complexity slightly increases with their order. An important property of the proposed formulae is that they work well close to the zero-offset and that they have exact long-offset asymptote. They may be less accurate for intermediate offsets (see the numerical examples), especially for offsets, for which ray- and phase-velocity vectors deviate significantly. In this way, the formulae behave like the generalized approximation of Fomel and Stovas (2010), see their tests in Golikov and Stovas (2012). Besides VTI media, the proposed formulae are also applicable to transversely isotropic media with horizontal axis of symmetry (HTI) or to orthorhombic media, in which the reflector coincides with one symmetry plane and the reflected ray is situated in another one.

In the following, the lower-case indices i, j, k, l, \dots take the values of 1,2,3, the upper-case indices I, J, K, L, \dots take the values of 1,2. The Einstein summation convention over repeated indices is used.

2 TRAVELTIME FORMULA

Let us consider the Cartesian coordinate system x_i , whose x_3 -axis is vertical and axes x_1 and x_2 are horizontal. We consider a homogeneous transversely isotropic medium with vertical axis of symmetry (VTI medium). The exact expression for the square of the travelttime of an unconverted reflected wave propagating in such a medium from source S to the reflector and then to receiver R , with both points S and R being situated at the same horizontal level, has then the form:

$$T^2(x) = \frac{4H^2 + x^2}{v^2(\mathbf{n})} . \quad (1)$$

Here x is the offset (distance between S and R ; along the x_1 -axis) and H is the depth of the horizontal reflector. $T = T(x)$ denotes the travelttime of the considered unconverted reflected wave; it is the function of the offset. Symbol $v = v(\mathbf{n})$ denotes the ray (sometimes called group) velocity, which is a function of the direction \mathbf{n} of slowness vector \mathbf{p} (or phase-velocity vector $\mathbf{c}(\mathbf{n})$). In the considered configuration $v(\mathbf{n})$ is the same along the down- and up-going part of the reflected ray.

We can express equation 1 using the notation common in moveout analysis:

$$\bar{x} = \frac{x}{2H} , \quad T_0 = \frac{2H}{V} . \quad (2)$$

Here \bar{x} is the normalized offset, V is the vertical phase velocity, $V = \alpha_0$ in case of P-waves and $V = \beta_0$ in case of SV-waves. It is equal to ray velocity in the vertical direction since it is the symmetry-axis direction. Symbol T_0 denotes the two-way zero-offset travelttime. Using 2, equation 1 can be expressed as:

$$T^2(\bar{x}) = V^2 T_0^2 \frac{1 + \bar{x}^2}{v^2(\mathbf{n})} . \quad (3)$$

In order to evaluate T^2 from equation 3, it is necessary to know the direction \mathbf{n} of the slowness vector. It may differ considerably from the direction \mathbf{N} of the ray velocity, which specifies the direction of the ray. We assume vector \mathbf{N} to be situated in the coordinate plane (x_1, x_3) and to have positive N_1 component. Vector \mathbf{N} can be easily determined from the geometry, which leads to equation 1. Because we consider a homogeneous VTI medium, it is not important if \mathbf{N} specifies the direction of the downgoing or upgoing part of the ray of a reflected wave. Let us consider the downgoing part, for which the N_1 and N_3 components of vector \mathbf{N} are positive. They can then be expressed in terms of the normalized offset \bar{x} as:

$$N_1 = \frac{\bar{x}}{\sqrt{1 + \bar{x}^2}} , \quad N_3 = \frac{1}{\sqrt{1 + \bar{x}^2}} . \quad (4)$$

It is relatively simple to determine the ray-velocity direction \mathbf{N} corresponding to a given slowness-vector direction \mathbf{n} . It is, however, quite complicated to determine \mathbf{n} for given \mathbf{N} . In fact, this problem is commonly addressed in two-point ray tracing in anisotropic media: in order to construct a ray between two specified points, one needs to find, at one of the points, the slowness vector corresponding to the ray connecting them. The problem simplifies if the anisotropy of the studied medium can be considered weak. Backus (1965) showed that in such a medium, for a given \mathbf{n} , the ray velocity $v(\mathbf{n})$ is equal to the phase velocity $c(\mathbf{n})$ in the first-order approximation with respect to the deviations of anisotropy from isotropy. In other words, the difference of $v(\mathbf{n})$ and $c(\mathbf{n})$ is of the second order. Remember that the direction \mathbf{N} of ray velocity generally differs from the direction \mathbf{n} of the phase velocity. Pšenčík and Vavryčuk (2002) and Farra (2004) confirmed Backus' (1965) observation and, in addition, they presented formulae relating \mathbf{N} and \mathbf{n} and showed that the difference between the directions of the ray-velocity and phase-velocity vectors, \mathbf{N} and \mathbf{n} , is of the first order. Neglecting this difference may thus have more important consequences than neglecting the difference of $v(\mathbf{n})$ and $c(\mathbf{n})$. To illustrate this, we perform two different tests to evaluate equation 3:

- 1) We ignore the difference between vectors \mathbf{n} and \mathbf{N} ;
- 2) We take the difference between vectors \mathbf{n} and \mathbf{N} into account.

All the above equations and discussions hold for both P and SV unconverted reflected waves. We concentrate now on P-waves. SV-waves will be treated later.

3 P-WAVE MOVEOUT

Let us start with introducing some relations, which are useful in the following considerations. First, let us introduce the equation for the square of the first-order P-wave phase velocity in a general weakly anisotropic medium (see, e.g., Pšenčík and Gajewski, 1998):

$$c^2(\mathbf{n}) = B_{33}(\mathbf{n}) = a_{ijkl}n_jn_l n_i n_k . \quad (5)$$

Here a_{ijkl} are density-normalized elastic moduli. Symbol B_{33} denotes an element of the symmetric matrix $\mathbf{B}(\mathbf{n})$, whose diagonal elements contain zero- and first-order terms and off-diagonal elements contain only first-order terms with respect to the deviations of anisotropy from isotropy. The elements of matrix $\mathbf{B}(\mathbf{n})$ are given by the formula (Farra and Pšenčík, 2003):

$$B_{mn}(\mathbf{n}) = a_{ijkl}n_jn_l e_{mi}e_{nk} . \quad (6)$$

The symbol n_i denotes the i -th component of the vector \mathbf{n} specifying the direction of the slowness vector. Symbol e_{ij} denotes the j -th component of vector \mathbf{e}_i . Vectors \mathbf{e}_i form an orthonormal triplet, in which $\mathbf{e}_3 = \mathbf{n}$. Vector \mathbf{e}_3 represents the zero-order approximation of the P-wave polarization vector. Vectors \mathbf{e}_K can be chosen arbitrarily in the plane perpendicular to \mathbf{n} . In the VTI medium, specifically in the (x_1, x_3) plane, equation 5 reduces to (see, e.g., Pšenčík and Farra, 2005):

$$c^2(\mathbf{n}) = \alpha_0^2[1 + 2(\delta_W - \epsilon_W)n_1^2n_3^2 + 2\epsilon_Wn_1^2] . \quad (7)$$

Parameters $\epsilon_W = (A_{11} - \alpha_0^2)/2\alpha_0^2$ and $\delta_W = (A_{13} + 2A_{55} - \alpha_0^2)/\alpha_0^2$ are the weak anisotropy (WA) parameters, which represent linearized Thomsen's (1986) parameters. For the definition of the WA parameters, see Farra and Pšenčík (2003). For $\alpha_0^2 = A_{33}$ used in 7, ϵ_W is identical to Thomsen's ϵ and δ_W is linearized Thomsen's δ . Symbols $A_{\beta\gamma}$ ($\beta, \gamma = 1, 2, \dots, 6$) denote density-normalized elastic moduli in the Voigt notation. We can see from equation 7 that the square of the first-order P-wave phase velocity c depends on three parameters of the medium: α_0 , ϵ_W and δ_W , and on the direction of slowness vector \mathbf{n} .

In the following, we shall need an estimate of the difference between vectors \mathbf{n} and \mathbf{N} , and an estimate of the change of the square of the phase velocity due to the replacement of $c^2(\mathbf{n})$ by $c^2(\mathbf{N})$. These problems were studied by Pšenčík and Vavryčuk (2002) and Farra (2004). In the following, we prefer to use the formulae of Farra (2004) because they are more accurate than those of Pšenčík and Vavryčuk (2002). For P-waves in a weakly anisotropic medium of arbitrary symmetry, the difference $\Delta\mathbf{N}$ between the vectors \mathbf{N} and \mathbf{n} ,

$$\Delta\mathbf{N}(\mathbf{n}) = \mathbf{N}(\mathbf{n}) - \mathbf{n} \quad (8)$$

is

$$\Delta\mathbf{N}(\mathbf{n}) = 2c^{-2}(\mathbf{n})B_{I3}(\mathbf{n})\mathbf{e}_I(\mathbf{n}) . \quad (9)$$

The fact that the right-hand side of equation 9 is of the first order implies that the difference between vectors \mathbf{n} and \mathbf{N} is also of the first order. The components of the two vectors can, therefore, be interchanged within the first-order approximation everywhere, where they are multiplied by some first-order quantity. Thus, within the first-order approximation, we have, for example, $\mathbf{B}(\mathbf{n}) = \mathbf{B}(\mathbf{N})$. We use this property broadly in the following analysis. Note that taking into account 5, it implies, for example, $c^2(\mathbf{n}) = c^2(\mathbf{N})$.

All quantities appearing on the right-hand side of equation 9 have been defined above. Equations 8 and 9 simply follow from equation (22) of Farra (2004) if we take into account that, to the first order, $v(\mathbf{n}) = c(\mathbf{n})$. With 8 and 9 we can seek the relation between $c^2(\mathbf{n})$ and $c^2(\mathbf{N})$. As shown in 7, a simple expression for $c^2(\mathbf{n})$ is available, but \mathbf{n} is unknown. From the configuration leading to equation 1 we know \mathbf{N} , but not \mathbf{n} . From 5 and 8, we simply get

$$c^2(\mathbf{n}) = c^2(\mathbf{N}) - \Delta c^2(\mathbf{N}) , \quad (10)$$

where

$$\Delta c^2(\mathbf{N}) = 4a_{ijkl}\Delta N_j N_l N_i N_k \quad (11)$$

is of second order. Inserting $\Delta\mathbf{N}$ given in 9 to 11 and using 6, we get

$$\Delta c^2(\mathbf{N}) = 8c^{-2}(\mathbf{N})B_{I3}(\mathbf{N})a_{ijkl}e_{Ij}N_l N_i N_k = 8c^{-2}(\mathbf{N})[B_{13}^2(\mathbf{N}) + B_{23}^2(\mathbf{N})] . \quad (12)$$

Hence, see 10,

$$c^2(\mathbf{n}) = c^2(\mathbf{N}) - 8c^{-2}(\mathbf{N})[B_{13}^2(\mathbf{N}) + B_{23}^2(\mathbf{N})] . \quad (13)$$

It remains to determine the expression for the square of the ray velocity $v^2(\mathbf{n})$ appearing in 3 in terms of $c^2(\mathbf{n})$. We use the first-order equation (22) of Farra (2004) relating the ray-velocity $\mathbf{v}(\mathbf{n})$ and phase-velocity $\mathbf{c}(\mathbf{n}) = c(\mathbf{n})\mathbf{n}$ vectors for a given \mathbf{n} :

$$\mathbf{v}(\mathbf{n}) = c(\mathbf{n})\mathbf{n} + 2c^{-1}(\mathbf{n})[B_{13}(\mathbf{n})\mathbf{e}_1(\mathbf{n}) + B_{23}(\mathbf{n})\mathbf{e}_2(\mathbf{n})] . \quad (14)$$

From 14 we simply obtain the expression for the square of the first-order ray velocity:

$$v^2(\mathbf{n}) = c^2(\mathbf{n}) + 4c^{-2}(\mathbf{n})[B_{13}^2(\mathbf{n}) + B_{23}^2(\mathbf{n})] . \quad (15)$$

We can now insert $c^2(\mathbf{n})$ from 13 into 15 to obtain the final expression for the square of the first-order ray velocity:

$$v^2(\mathbf{n}) = c^2(\mathbf{N}) - 4c^{-2}(\mathbf{N})[B_{13}^2(\mathbf{N}) + B_{23}^2(\mathbf{N})] . \quad (16)$$

The accuracy of the moveout formulae can be further enhanced by replacing the first-order expression for the phase velocity squared in 16 by its second-order expression (Farra, 2001). Generalized equation 16 then yields the expression for the square of the second-order ray velocity:

$$v^2(\mathbf{n}) = c^2(\mathbf{N}) + c^{-2}(\mathbf{N})[B_{13}^2(\mathbf{N}) + B_{23}^2(\mathbf{N})][(1 - r^2)^{-1} - 4] . \quad (17)$$

In 17, $r = \beta_0/\alpha_0$, $\alpha_0^2 = A_{33}$ and $\beta_0^2 = A_{55}$.

Let us emphasize that all the above formulae, except 7, hold for weak anisotropy of arbitrary symmetry.

Finally, let us specify the elements B_{I3} of the matrix \mathbf{B} , which appear in 16 or 17, for the VTI medium. As Pšenčík and Gajewski (1998), we consider vectors \mathbf{e}_1 and \mathbf{e}_2 chosen so that \mathbf{e}_2 is perpendicular to plane (x_1, x_3) and vectors \mathbf{e}_i form a right-handed orthonormal triplet. In the studied plane (x_1, x_3) :

$$B_{13}(\mathbf{N}) = \alpha_0^2 N_1 N_3 [\delta_W - 2(\delta_W - \epsilon_W) N_1^2] , \quad B_{23} = 0 . \quad (18)$$

Note that, as shown by Farra and Pšenčík (2003), the term $B_{13}^2(\mathbf{N}) + B_{23}^2(\mathbf{N})$ appearing in 13, 15, 16 and 17 does not depend on the choice of vectors \mathbf{e}_I . Also note that equation 16 can serve as an alternative three-parametric expression of the ray velocity (Fomel, 2003).

3.1 Case 1

If we specify $V = \alpha_0$ and ignore the difference between vectors \mathbf{n} and \mathbf{N} , then in the first-order approximation, $v^2(\mathbf{n}) = c^2(\mathbf{N})$, and equation 3 can be expressed as follows:

$$T^2(\bar{x}) = \alpha_0^2 T_0^2 \frac{1 + \bar{x}^2}{c^2(\mathbf{N})} . \quad (19)$$

Inserting 7 and 4 into 19, after some algebra yields, the first-order expression for T^2 :

$$T^2(\bar{x}) = T_0^2 \frac{(1 + \bar{x}^2)^3}{P(\bar{x})} . \quad (20)$$

Here

$$P(\bar{x}) = (1 + \bar{x}^2)^2 + 2\delta_W \bar{x}^2 + 2\epsilon_W \bar{x}^4 \quad (21)$$

is polynomial containing terms of zero and first order in the WA parameters. For zero offset, equation 20 yields correctly the square of the two-way zero-offset travelttime T_0 .

For long offsets, $\lim_{x \rightarrow \infty} T^2(x)/x^2$ yields the correct value c_H^{-2} , where $c_H^2 = \alpha_0^2(1 + 2\epsilon_W)$ is the phase velocity in the horizontal direction, see 7.

Separating the terms emphasizing short and long offsets, 20 can be expressed in the following form:

$$T^2(\bar{x}) = T_0^2 \left[1 + (1 - 2\delta_W)\bar{x}^2 + 2\bar{x}^4 \frac{\delta_W - \epsilon_W + 2\delta_W^2 + (\delta_W - \epsilon_W + 2\delta_W\epsilon_W)\bar{x}^2}{P(\bar{x})} \right]. \quad (22)$$

We can see that equation 22 contains also some second-order terms. Neglecting them leads to a simplified expression:

$$T^2(\bar{x}) = T_0^2 \left[1 + (1 - 2\delta_W)\bar{x}^2 + 2\bar{x}^4 \frac{(\delta_W - \epsilon_W)}{1 + \bar{x}^2} \right]. \quad (23)$$

This expression is identical (if we neglect differences between δ_W and δ) with the weak-anisotropy approximation of the nonhyperbolic moveout (4.20) of Tsvankin (2001). It is obvious that the omission of the second-order terms in equation 22 reduces the accuracy of the already inaccurate formula (the difference between vectors \mathbf{n} and \mathbf{N} was neglected) for intermediate and long offsets. Indeed, the $\lim_{x \rightarrow \infty} T^2(x)/x^2$ for 23 yields $\alpha_0^{-2}(1 - 2\epsilon_W)$, which represents the first-order approximation of the inverse square of the exact horizontal phase velocity. It differs from the exact value, indicating incorrect asymptotical behaviour of the formula 23 for long offsets, especially when ϵ_W is larger.

3.2 Case 2

We now take into account the difference between vectors \mathbf{n} and \mathbf{N} , specifically we take into account equation 16. Inserting 16 into 3 and considering 7 and 4, after some algebra yields a more accurate first-order expression for T^2 than 20:

$$T^2(\bar{x}) = T_0^2 \frac{(1 + \bar{x}^2)^3 P(\bar{x})}{P^2(\bar{x}) - Q^2(\bar{x})}. \quad (24)$$

In 24, polynomial $P(\bar{x})$ is given in 21 and $Q(\bar{x})$ reads:

$$Q(\bar{x}) = 2\bar{x}[2\epsilon_W\bar{x}^2 + \delta_W(1 - \bar{x}^2)]. \quad (25)$$

Polynomial $P(\bar{x})$ contains terms of zero and first order in the WA parameters while polynomial $Q(\bar{x})$ contains only terms of the first order. Thus if we wish to ignore the second-order terms in 24, $Q^2(\bar{x})$ must be neglected with respect to $P^2(\bar{x})$, and 24 reduces to 20. Although 24 is a first-order expression like 20, it is more accurate because it takes into account the different directions of \mathbf{n} and \mathbf{N} , see 9, and the difference between the ray and phase velocities squared, see 15.

The accuracy of 24 can be further increased by using the second-order expression for the phase velocity 17, inserting it into 3 and taking into account 7 and 4. Then, after some algebra, we obtain the second-order expression for T^2 :

$$T^2(\bar{x}) = T_0^2 \frac{(1 + \bar{x}^2)^3 P(\bar{x})}{P^2(\bar{x}) + aQ^2(\bar{x})}. \quad (26)$$

Here $a = (r^2 - 3/4)/(1 - r^2)$.

Approximation 24 depends on four parameters: two-way zero-offset traveltime T_0 , related to α_0 , the depth H of the reflector and two WA parameters ϵ_W and δ_W . In addition to these parameters, approximation 26 depends on an additional parameter r , the ratio of the S- and P-wave velocities. For realistic values of r , the value of a varies only little (for r between 0.1 and 0.5, the value of a varies between -0.75 and -0.65). Numerical tests with 26 confirm that the dependence of 26 on r is very weak and thus r need not be considered as a free parameter. Both equations 24 and 26 display correct asymptotical behaviour for long offsets.

It is important to emphasize that the above moveout formulae yield the NMO velocity v_{NMO}^W whose accuracy depends on the accuracy of the corresponding formula. For example, equation 26 yields $(v_{NMO}^W)^2 = \alpha_0^2(1 - 2\delta_W - 4a\delta_W^2)^{-1}$, where $a = (r^2 - 3/4)/(1 - r^2)$ again. It is easy to show that it represents the second-order approximation of the square of the exact NMO velocity $v_{NMO}^2 = \alpha_0^2(1 + 2\delta)$, where δ is the non-linearized Thomsen's parameter. In a similar way we can obtain first-order approximations of NMO velocity from formulae 20 and 24. Coefficients of x^4 in the Taylor expansion of $T^2(x)$ in x^2 obtained from equations 20 and 24 are the first-order and from equation 26 the second-order approximations of the exact coefficient.

The formulae derived in this section hold also for the case of the reflected ray situated in a vertical symmetry plane of an HTI medium or in one symmetry plane of an orthorhombic medium and the reflector in another. Only the appropriate parameters ϵ_W and δ_W must be considered. It is worth mentioning that the formulae could also be generalized to the case of a reflection from an interface underlying an HTI medium with arbitrarily oriented axis of symmetry, or from an interface coinciding with a symmetry plane of a medium of orthorhombic (applicability is more general than with the presented formulae; in this case rays of the reflected wave do not need to be situated in one of the remaining symmetry planes) or even monoclinic symmetry.

4 SV-WAVE MOVEOUT

Without loss of generality, we consider only one of the two S-waves and denote it S1. The equation for the square of its first-order phase velocity in a weakly anisotropic medium of arbitrary symmetry reads (see, e.g., Farra, 2004):

$$c^2(\mathbf{n}) = B_{11}(\mathbf{n}) = a_{ijkl}n_jn_l e_{1i}e_{1k} . \quad (27)$$

Here, $B_{11}(\mathbf{n})$ is an element of matrix \mathbf{B} , see 6. Symbols e_{1i} denote the components of unit vector \mathbf{e}_1 from the orthonormal triplet \mathbf{e}_1 , \mathbf{e}_2 and \mathbf{n} . Vectors \mathbf{e}_1 and \mathbf{e}_2 are chosen so that the element $B_{12}(\mathbf{n})$ of the matrix \mathbf{B} is zero, i.e., $B_{12}(\mathbf{n}) = 0$. Vector \mathbf{e}_1 then also represents the zero-order approximation of the S1-wave polarization vector.

The difference $\Delta\mathbf{N}$ between the vectors \mathbf{N} and \mathbf{n} of the S1 wave in a weakly anisotropic medium of arbitrary symmetry reads:

$$\Delta\mathbf{N}(\mathbf{n}) = c^{-2}(\mathbf{n})[(a_{ijkl}n_l e_{1i}e_{1k}e_{1j} - B_{13}(\mathbf{n}))\mathbf{e}_1(\mathbf{n}) + (a_{ijkl}n_l e_{1i}e_{1k}e_{2j})\mathbf{e}_2(\mathbf{n})] . \quad (28)$$

This simply follows from the results derived by Farra (2004).

In the VTI medium, for vector $\mathbf{e}_1(\mathbf{n})$ situated in the (x_1, x_3) plane, $\mathbf{e}_1(\mathbf{n}) = (n_3, 0, -n_1)$, the expression for the square of the first-order S1-wave phase velocity 27 reduces to the equation for the square of the SV-wave phase velocity:

$$c^2(\mathbf{n}) = \beta_0^2(1 + 2\sigma_W n_1^2 n_3^2) , \quad (29)$$

see, e.g., Farra (2001). Symbol σ_W is analogous to Tsvankin's (2001) parameter σ , here, however, specified by the WA parameters:

$$\sigma_W = r^{-2}(\epsilon_W - \delta_W) . \quad (30)$$

As before $r = \beta_0/\alpha_0$, $\alpha_0^2 = A_{33}$, $\beta_0^2 = A_{55}$ and ϵ_W and δ_W are linearized Thomsen's (1986) parameters. Equation 28 can be expressed as:

$$\Delta\mathbf{N}(\mathbf{n}) = 2c^{-2}(\mathbf{n})E_I(\mathbf{n})\mathbf{e}_I(\mathbf{n}) . \quad (31)$$

For the VTI medium, the first-order terms $E_I(\mathbf{n})$ in 31 read:

$$E_1(\mathbf{n}) = \beta_0^2\sigma_W n_1 n_3 (n_3^2 - n_1^2) , \quad E_2(\mathbf{n}) = 0 . \quad (32)$$

Expression 31 is needed for the estimate of the effect on $c^2(\mathbf{n})$ of the replacement of \mathbf{n} by \mathbf{N} . By inserting $\mathbf{n} = \mathbf{N} - \Delta\mathbf{N}$ into 29, we get $c^2(\mathbf{n}) = c^2(\mathbf{N}) - \Delta c^2(\mathbf{N})$, see equation 10. From 29 we then get

$$\Delta c^2(\mathbf{N}) = 4\beta_0^2\sigma_W N_1 N_3 (N_3 \Delta N_1 + N_1 \Delta N_3) , \quad (33)$$

which is the second-order quantity. If we insert $\Delta\mathbf{N}$ from 31 into 33, and the result to equation 10, we arrive at:

$$c^2(\mathbf{n}) = c^2(\mathbf{N}) - 8c^{-2}(\mathbf{N})[E_1^2(\mathbf{N}) + E_2^2(\mathbf{N})] . \quad (34)$$

This is an equation for the square of the SV-wave phase velocity in VTI media, analogous to equation 13 for P-waves in weakly anisotropic media of arbitrary symmetry.

It remains to express the square of the SV-wave ray-velocity vector $\mathbf{v}(\mathbf{n})$ appearing in 3 in terms of $c^2(\mathbf{n})$. We can use equation 24 of Farra (2004), relating ray- and phase-velocity vectors for a given \mathbf{n} , and specify it for a VTI medium:

$$\mathbf{v}(\mathbf{n}) = c(\mathbf{n})\mathbf{n} + 2c^{-1}(\mathbf{n})[E_1(\mathbf{n})\mathbf{e}_1(\mathbf{n}) + E_2(\mathbf{n})\mathbf{e}_2(\mathbf{n})] . \quad (35)$$

Squaring the vector $\mathbf{v}(\mathbf{n})$ given in 35, we obtain

$$v^2(\mathbf{n}) = c^2(\mathbf{n}) + 4c^{-2}(\mathbf{n})[E_1^2(\mathbf{n}) + E_2^2(\mathbf{n})] . \quad (36)$$

Substitution of $c^2(\mathbf{n})$ from 34 to 36 yields the final result:

$$v^2(\mathbf{n}) = c^2(\mathbf{N}) - 4c^{-2}(\mathbf{N})[E_1^2(\mathbf{N}) + E_2^2(\mathbf{N})] . \quad (37)$$

Note that 37 with $E_I(\mathbf{N})$ given in 32 represents a two-parametric expression for the ray velocity.

The accuracy of the SV-wave moveout formulae can further be enhanced by replacing the first-order expression for the SV-wave phase velocity squared in 37 by its second-order expression (Farra, 2001). Considering $E_2(\mathbf{n}) = 0$ as given in the second equation of 32, generalized equation 37 becomes:

$$v^2(\mathbf{n}) = c^2(\mathbf{N}) - c^{-2}(\mathbf{N}) \left[\frac{r^2}{1-r^2} F^2(\mathbf{N}) + 4E_1^2(\mathbf{N}) \right]. \quad (38)$$

Here

$$F(\mathbf{N}) = \alpha_0^2 N_1 N_3 [\epsilon_W - r^2 \sigma_W (N_3^2 - N_1^2)]. \quad (39)$$

4.1 Case 1

If we specify $V = \beta_0$ and ignore the difference between vectors \mathbf{n} and \mathbf{N} , then in the first-order approximation, $v^2(\mathbf{n}) = c^2(\mathbf{N})$, and equation 3 can be expressed as:

$$T^2(\bar{x}) = \beta_0^2 T_0^2 \frac{(1 + \bar{x}^2)^3}{c^2(\mathbf{N})}. \quad (40)$$

Inserting 29 and 4 into 40 yields, after some simple algebra:

$$T^2(\bar{x}) = T_0^2 \frac{(1 + \bar{x}^2)^3}{P(\bar{x})}. \quad (41)$$

Here

$$P(\bar{x}) = (1 + \bar{x}^2)^2 + 2\sigma_W \bar{x}^2 \quad (42)$$

is polynomial, which contains terms of zero and first order in the WA parameters. Equation 41 yields correctly T_0^2 for the zero offset. For long offsets, it has the correct asymptote related to phase velocity $c_H = \beta_0$ in the horizontal direction.

Separating the terms emphasizing short and long offsets, we can modify 41 to the following form:

$$T^2(\bar{x}) = T_0^2 \left[1 + (1 - 2\sigma_W) \bar{x}^2 + 2\sigma_W \bar{x}^4 \frac{1 + 2\sigma_W + \bar{x}^2}{P(\bar{x})} \right]. \quad (43)$$

Neglecting second-order terms in 43 leads to a simplified expression

$$T^2(\bar{x}) = T_0^2 \left[1 + (1 - 2\sigma_W) \bar{x}^2 + \frac{2\sigma_W \bar{x}^4}{1 + \bar{x}^2} \right] \quad (44)$$

with reduced accuracy, especially for intermediate offsets. For large offsets, its accuracy, however, improves since the formula yields exact value β^{-2} of the inverse square of the phase velocity in the horizontal direction indicating a correct infinite-offset asymptote. Note that this was not the case with a similar equation for the P-wave moveout, 23. In case of P-waves, 23 yields only approximate value of the inverse square of the exact horizontal phase velocity.

4.2 Case 2

We now take into account the difference between vectors \mathbf{n} and \mathbf{N} , specifically we take into account equation 37. Inserting 37 into 3 and considering 29 and 4, after some algebra yields a more accurate first-order expression for SV-wave T^2 than 41:

$$T^2(\bar{x}) = T_0^2 \frac{(1 + \bar{x}^2)^3 P(\bar{x})}{P^2(\bar{x}) - Q^2(\bar{x})} . \quad (45)$$

In 45, polynomial $P(\bar{x})$ is given in 42 and $Q(\bar{x})$ is given by:

$$Q(\bar{x}) = 2\sigma_W \bar{x}(1 - \bar{x}^2) . \quad (46)$$

Polynomial $P(\bar{x})$ contains zero- and first-order terms with respect to the WA parameters, while $Q(\bar{x})$ contains, as in the case of P-waves, only a first-order term. If we wish to ignore the second-order terms in 45, $Q^2(\bar{x})$ must be neglected with respect to $P^2(\bar{x})$, and 45 reduces to 41. Although 45 is a first-order expression like 41, it is more accurate because it takes into account the different directions of \mathbf{n} and \mathbf{N} , see 31, and the difference between the ray and phase velocities squared, see 36.

The accuracy of 45 can be increased by using the second-order expression for the square of the phase velocity 38. Inserting it into 3 and taking into account 29 and 4, after some algebra yields the second-order expression for T^2 :

$$T^2(\bar{x}) = T_0^2 \frac{(1 + \bar{x}^2)^3 P(\bar{x})}{P^2(\bar{x}) - Q^2(\bar{x}) - (1 - r^2)^{-1} R^2(\bar{x})} . \quad (47)$$

Here $R(\bar{x})$ reads:

$$R(\bar{x}) = r^{-1} \bar{x} [2\epsilon_W \bar{x}^2 + \delta_W (1 - \bar{x}^2)] . \quad (48)$$

We can see that $R(\bar{x})$ contains only first-order terms with respect to the WA parameters. Thus if we wish to neglect the second-order terms in 47, equation 47 reduces to 41 again. It remains to note that both equations 45 and 47 have correct infinite-offset asymptotes.

As in the case of P-waves, the formulae derived in this section hold also for the case of the reflected ray situated in the vertical symmetry plane of an HTI medium or in one symmetry plane of an orthorhombic medium and the reflector in another, if the appropriate σ_W parameter is considered.

Let us also emphasize that the SV-wave moveout formulae presented in this paper yield approximate NMO velocities. Their accuracy depends on the accuracy of the formula, from which is the given NMO velocity derived. For example, equation 47 yields $(v_{NMO}^W)^2 = \beta_0^2 [1 - 2\sigma_W + 4\sigma_W^2 + \delta_W^2 r^{-2} (1 - r^2)^{-1}]^{-1}$. As in the P-wave case, it is easy to show that this is the second-order approximation of the square of the exact NMO velocity $v_{NMO}^2 = \beta_0^2 (1 + 2\sigma)$, where σ is specified by non-linearized Thomsen's parameters. NMO velocities derived from formulae 41 and 45 represent first-order approximations of the exact NMO velocity. Coefficients of x^4 in the Taylor expansion of $T^2(x)$ in x^2 obtained from equations 41 and 45 are the first-order and from equation 47 the second-order approximations of the exact coefficient.

5 REFERENCE MOVEOUT FORMULAE

To estimate the accuracy of the above formulae for T^2 , we compare their results with the results of commonly used formulae. In case of P-waves, we use the long-spread moveout equation (Tsvankin, 2001, equation 4.23, see also Alkhalifah and Tsvankin, 1995) derived in the quasi-acoustic approximation, i.e., assuming $\beta_0 = 0$. With the notation 2, the long-spread moveout equation for P-waves reads

$$T^2(\bar{x}) = T_0^2 \left(1 + R_\delta \bar{x}^2 - \frac{2\eta R_\delta^2 \bar{x}^4}{1 + S R_\delta \bar{x}^2} \right). \quad (49)$$

Here

$$R_\delta = (1 + 2\delta)^{-1}, \quad S = R_\delta(1 + 2\epsilon), \quad (50)$$

where ϵ and δ are Thomsen's (1986) parameters (non-linearized), $\eta = R_\delta(\epsilon - \delta)$, see Tsvankin (2001).

In case of SV-waves, we use the rational approximation of Alkhalifah and Tsvankin (1995), see Stovas (2010, equation 4). The rational approximation for SV-waves with the notation 2 has the form:

$$T^2(\bar{x}) = T_0^2 \left(1 + R_\sigma \bar{x}^2 + \frac{A R_\sigma^2 \bar{x}^4}{1 + B R_\sigma \bar{x}^2} \right). \quad (51)$$

The coefficients A , B and R_σ in 51 read:

$$A = 2\sigma B, \quad B = R_\sigma^2 \frac{1 - r^2 + 2\delta}{1 - r^2}, \quad R_\sigma = (1 + 2\sigma)^{-1}, \quad (52)$$

where $\sigma = r^{-2}(\epsilon - \delta)$ and $r^2 = \beta_0^2/\alpha_0^2$. The meaning of all other variables is the same as in 49.

6 TESTS OF ACCURACY

Here we test the proposed formulae, specifically 20, 24, 26, and the reference formula 49 for P-waves and 41, 45, 47 and the reference formula 51 for SV-waves. We check the relative errors $(T - T_{ex})/T_{ex} \times 100\%$, where T_{ex} denotes the traveltimes calculated using the package ANRAY (Gajewski and Pšenčík, 1990), which we consider exact. We test the above formulae on models with varying anisotropy strength, used by Stovas (2010) and Tsvankin (2001). The anisotropy strength is defined as $2(V_{max} - V_{min})/(V_{max} + V_{min}) \times 100\%$. The models considered are the Limestone model, whose P-wave and SV-wave anisotropy are $\sim 8\%$ and $\sim 5\%$, respectively, the Greenhorn shale model with a P-wave anisotropy of $\sim 26\%$, the Mesaverde mudshale and the Hard shale models, both with an SV-wave anisotropy of $\sim 12\%$. The parameters of all four models are given in Table 1.

In Figure 1, we show the P-wave results for the weakly anisotropic Limestone model. We start with the comparison of the exact (black) and first-order (red) P-wave phase

Model	α_0 (km/s)	β_0 (km/s)	ϵ_W	δ_W	ϵ	δ
Limestone	3.0	1.707	0.076	0.133	0.076	0.146
Greenhorn shale	3.094	1.51	0.256	-0.0523	0.256	-0.0505
Mesaverde mudshale	4.53	2.703	0.034	0.184	0.034	0.211
Hard shale	3.0	1.914	0.252	0.034	0.252	0.035

Table 1: Parameters of the models used. α_0 and β_0 - P- and S-wave velocities, ϵ_W and δ_W - WA parameters, ϵ and δ - Thomsen's parameters.

velocities as functions of the normalized offset \bar{x} in Figure 1a. We can see that the first-order phase-velocity formula works very well, the difference between both velocities is negligible, and both curves effectively coincide. On close inspection, we can see that the first-order phase velocity is always less than the exact one. This confirms the theoretical observation made, for example, by Farra and Pšenčík (2003). Note that the first-order and exact velocities are equal for the zero offset, which in the VTI medium corresponds to the longitudinal direction, in which P-wave is purely longitudinal and S-wave purely transverse (Helbig, 1993). Similarly, both velocities converge to each other with increasing offset because the horizontal direction represents another longitudinal direction, in which they coincide. The curves of the exact (black) P-wave ray and phase (red) velocities in Figure 1b behave in a similar way. Here, however, a small difference between them is observable. The phase velocity is less than the ray velocity. In Figure 1c, we can see the variation of the angle between the ray- and phase-velocity vectors, i.e. between vectors \mathbf{N} and \mathbf{n} , as a function of the normalized offset \bar{x} . The black curve shows the angle between the exact vectors, the red curve between their first-order approximations. Both curves are effectively identical. We can see that vectors \mathbf{N} and \mathbf{n} coincide for the zero offset and approach each other for offsets increasing to infinity, which is the consequence of the fact that B_{13} in 18 is zero for $N_1 = 0$ or $N_3 = 0$, and thus $\Delta\mathbf{N}(\mathbf{n})$ in 9 is zero too. The most important feature of this figure is the magnitude of the angle between the two vectors for small offsets. Although the anisotropy is weak, the maximum difference between \mathbf{N} and \mathbf{n} is nearly 5° . This difference is responsible for the worse performance of the first-order moveout formulae for short offsets. If neglected, as in the case of equation 20, it can lead to a further decrease of the accuracy of the approximate formulae for the corresponding offsets. This can be seen in Figure 1d.

Figure 1d shows the relative P-wave traveltimes errors. The noisy character of the curves is caused by the two-point ray tracing procedure used for the reference traveltimes computations in the package ANRAY. The approximate traveltimes curves are smooth. The red curve represents the relative P-wave traveltimes errors of the first-order formula 20. In 20, the difference between the directions of the ray- and phase-velocity vectors \mathbf{N} and \mathbf{n} was ignored. The interval of offsets with increased errors closely correlates with the interval of offsets with increased deviations of vectors \mathbf{N} and \mathbf{n} in Figure 1c. Outside the interval, we can see that the relative errors of formula 20 are negligible. They reach their maximum of approximately 0.28% in a very narrow region of small non-zero offsets. Their maximum is approximately comparable with the errors of the long-spread moveout formula 49 shown as the black curve. However, for normalized offsets $\bar{x} > 1.5$, equation 20 yields much better results than 49. The relative traveltimes errors of the first-order

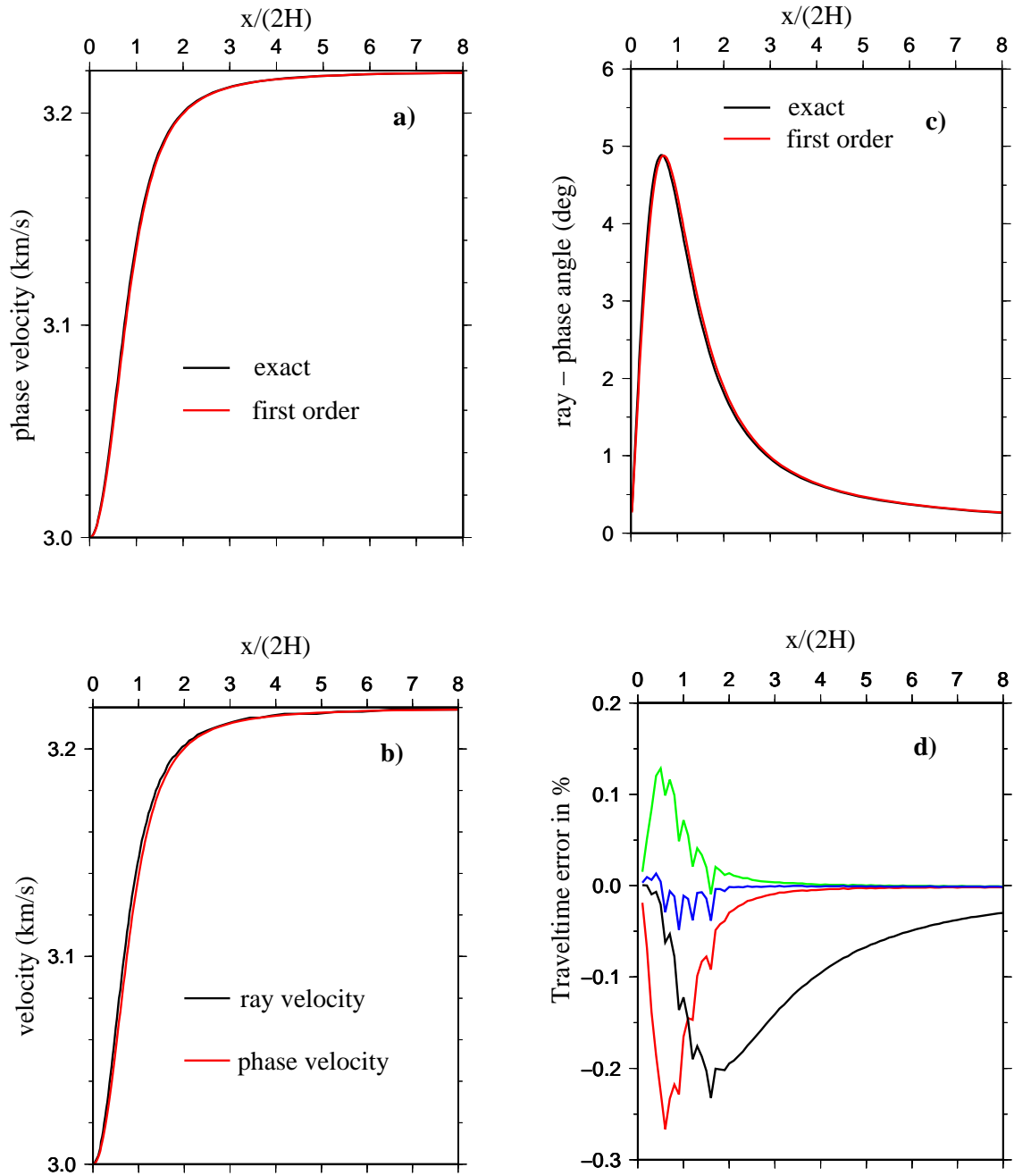


Figure 1: P-wave moveout in Limestone model, anisotropy $\sim 8\%$. Variation with the normalized offset $\bar{x} = x/2H$ of: a) Exact (black) and first-order (red) phase-velocities. b) Exact ray (black) and phase (red) velocities. c) Angular difference of exact (black) and first-order (red) ray- and phase-velocity directions \mathbf{N} and \mathbf{n} . d) Relative traveltime errors with traveltime calculated from the first-order equation 20 ignoring difference in directions of vectors \mathbf{N} and \mathbf{n} - red; from the first-order equation 24 taking into account different directions of \mathbf{N} and \mathbf{n} - green; the second-order equation 26 - blue; the long-spread moveout equation 49 - black.

formula 24, which takes into account the different directions of vectors \mathbf{N} and \mathbf{n} , are shown as the green curve. The maximum error is now considerably reduced, being less than 0.15%. The errors are effectively removed if the second-order equation 26, shown as the blue curve, is used. In this case, the maximum error is less than 0.03%.

Let us now test the approximate formulae on the Greenhorn shale model whose anisotropy is of about 26%, which cannot be considered weak.

In Figure 2a, we can see the comparison of the exact (black) and first-order (red) phase velocities as functions of the normalized offset \bar{x} . We can observe features similar to Figure 1a, but the differences of both velocities for intermediate offsets are now clearly visible. This means that due to strong anisotropy, the formula for the first-order phase velocity does not perform as well as it did in the previous case. In Figure 2b, we can observe substantially larger differences between the ray (black) and phase (red) velocities. Otherwise, the main features of the curves (coincidence for zero offset and mutual convergence for increasing offsets) are again preserved. Figure 2c shows that for an anisotropy of approximately 26%, the deviation of vectors \mathbf{N} and \mathbf{n} may reach 16° . We can also see that the interval of larger deviations of \mathbf{N} and \mathbf{n} extends to longer offsets. For small offsets, we can observe an interesting effect: change of mutual positions of vectors \mathbf{N} and \mathbf{n} at about $\bar{x} = 0.3$. It is consequence of the differences in angular variation of phase and ray velocities. Remember that vectors \mathbf{N} and \mathbf{n} are perpendicular to slowness and ray-velocity surfaces, respectively. The angle between \mathbf{N} and \mathbf{n} is zero at $\bar{x} \sim 0.3$; it corresponds to one of the longitudinal directions. For this offset, the term $\delta_W - 2(\delta_W - \epsilon_W)N_1^2$ appearing in B_{13} in equation 18 is zero. We can see that the value of this specific offset depends on the values of ϵ_W and δ_W . Consequently, $\Delta\mathbf{N}(\mathbf{n}) = 0$, see 9 and also $v^2(\mathbf{n}) = c^2(\mathbf{n})$, see 15. The deviations of the two vectors have again strong effect on traveltime errors, especially for intermediate offsets. We can see this in Figure 2d. We can see that equation 20, in which we neglected the deviation of \mathbf{N} and \mathbf{n} , yields errors, which can reach 2.5% (red). For $\bar{x} > 1$, equation 20 yields worse results than the long-spread formula 49 shown as the black curve. When the deviations of \mathbf{N} and \mathbf{n} are taken into account, see the green curve obtained from equation 24, the maximum error reduces below 2%. It further reduces, below about 0.5%, when we use the second-order equation 26. It is shown by blue curve in Figure 2d. Note that stronger anisotropy not only leads to greater maximum errors, but also to the extension of offsets with increased errors. This is caused by considerable deviations of vectors \mathbf{N} and \mathbf{n} , which extend to longer offsets (compare Figures 2c and 1c). The deviations of vectors \mathbf{N} and \mathbf{n} are caused by the large value of term $2\epsilon_W - \delta_W$, which plays a dominant role for long offsets, see equations 9 and 18. In the case of the Limestone model, this term is almost zero while for the Greenhorn shale model it is rather large, see Table 1. In any case, the maximum error of 0.5% in equation 26 for an anisotropy of about 26% seems to be a very good result.

In Figure 3, we again show the results for the Limestone model, but this time for the SV-wave. Although the anisotropy is weak ($\sim 5\%$), we can observe in Figure 3a, in contrast to Figure 1a, that for normalized offsets $\bar{x} \sim 1$, the exact (black) and first-order (red) SV-wave phase velocity curves differ slightly indicating that the first-order SV-wave phase-velocity formula yields slightly inaccurate results in this region. We can see that, in contrast to the P-wave case, the first-order phase velocity is always larger than the exact one. This agrees with the theoretical observation of Farra and Pšenčík (2003). Due to the existence of the longitudinal directions, the velocity curves in Figure 3a coincide for

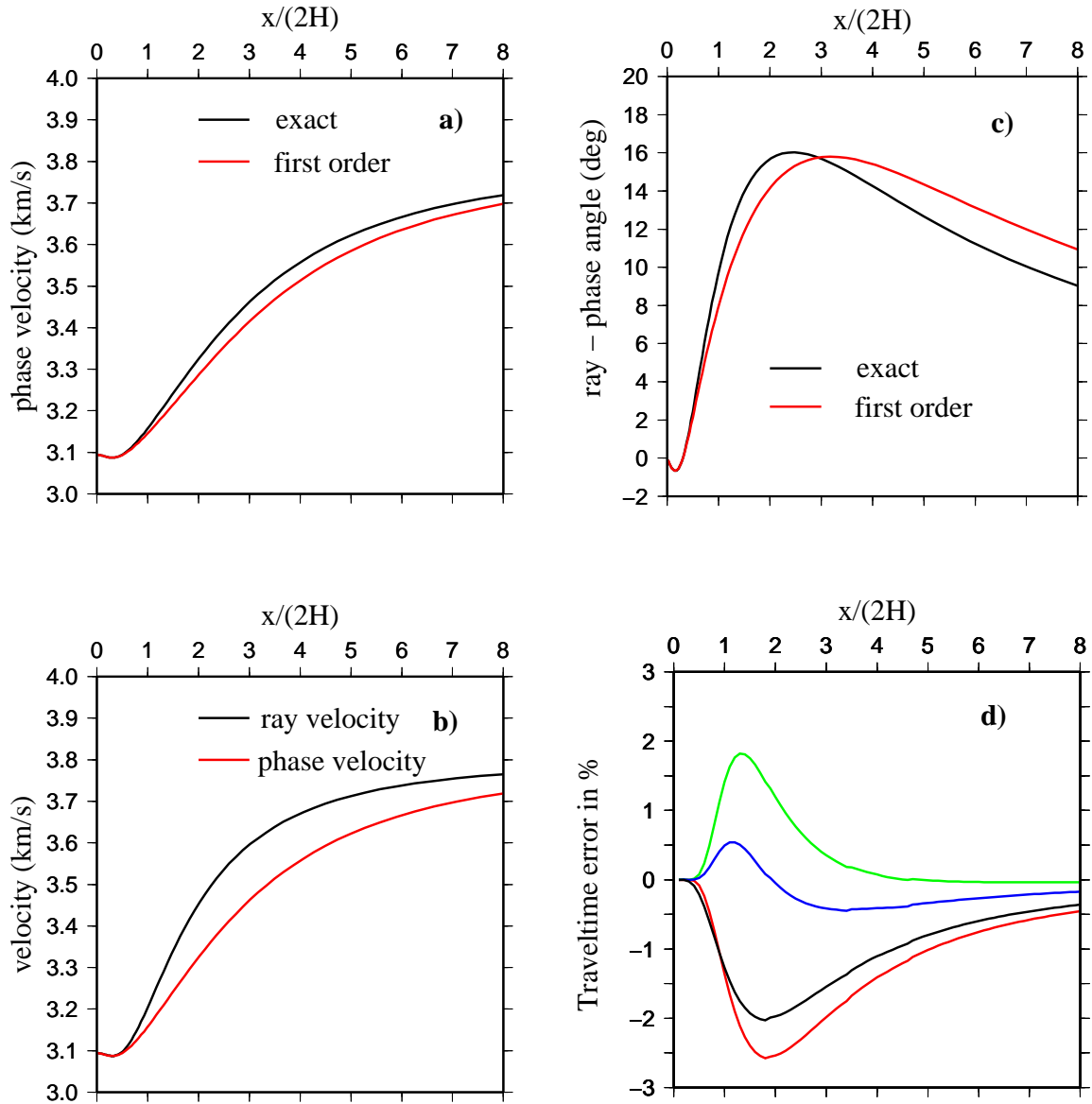


Figure 2: P-wave moveout in Greenhorn shale model, anisotropy $\sim 26\%$. Variation with the normalized offset $\bar{x} = x/2H$ of: a) Exact (black) and first-order (red) phase-velocities. b) Exact ray (black) and phase (red) velocities. c) Angular difference of exact (black) and first-order (red) ray- and phase-velocity directions \mathbf{N} and \mathbf{n} . d) Relative traveltimes errors with traveltimes calculated from the first-order equation 20 ignoring difference in directions of vectors \mathbf{N} and \mathbf{n} - red; from the first-order equation 24 taking into account different directions of \mathbf{N} and \mathbf{n} - green; the second-order equation 26 - blue; the long-spread moveout equation 49 - black.

the zero offset and converge to each other for increasing offsets. The exact SV-wave ray (black) and phase (red) velocities in Figure 3b differ for offsets $\bar{x} > 1$. As in the P-wave

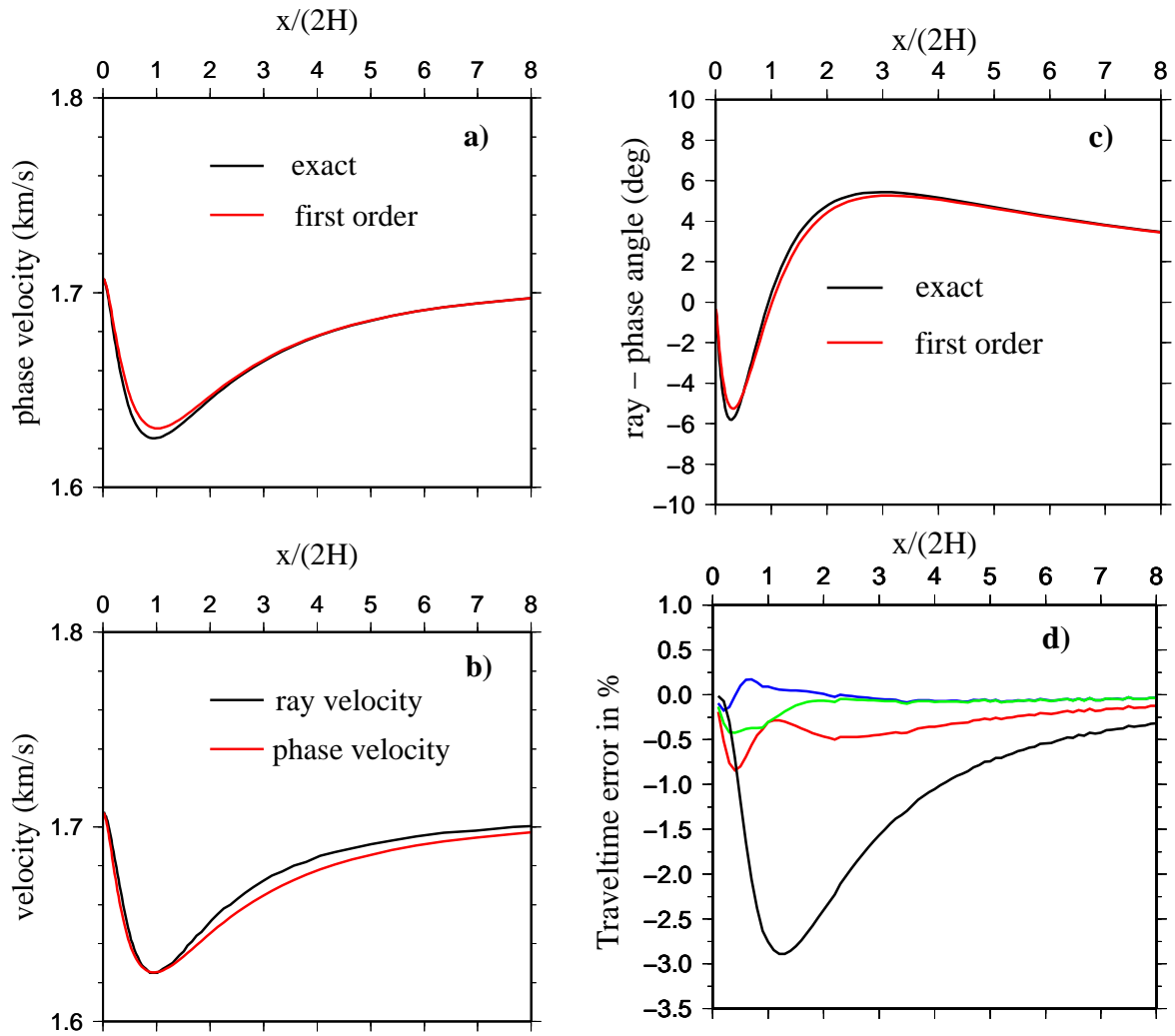


Figure 3: SV-wave moveout in Limestone model, anisotropy $\sim 5\%$. Variation with the normalized offset $\bar{x} = x/2H$ of: a) Exact (black) and first-order (red) phase-velocities. b) Exact ray (black) and phase (red) velocities. c) Angular difference of exact (black) and first-order (red) ray- and phase-velocity directions \mathbf{N} and \mathbf{n} . d) Relative traveltime errors with traveltime calculated from the first-order equation 41 ignoring difference in directions of vectors \mathbf{N} and \mathbf{n} - red; from the first-order equation 45 taking into account different directions of \mathbf{N} and \mathbf{n} - green; the second-order equation 47 - blue; the rational approximation 51 - black.

case, the ray velocity is, of course, always greater than or equal to the phase velocity. Although the SV-wave anisotropy is weaker than P-wave anisotropy, the deviations of vectors \mathbf{N} and \mathbf{n} , shown in Figure 3c, reach larger values than in the P-wave case: nearly 6° . Note that the first-order (red) curve approximates the exact (black) one very well. Due to the zero values of $E_1(\mathbf{n})$ in 32 for $n_1 = 0$ or $n_3 = 0$, which correspond to the vertical and

horizontal directions, the deviations are zero for the zero offset and converge to zero when the offsets increase to infinity. For $\bar{x} = 1$ we can observe the exchange of mutual positions of vectors \mathbf{N} and \mathbf{n} . The effect is more pronounced here than in Figure 2c. The offset $\bar{x} = 1$ corresponds to $n_3^2 - n_1^2 = 0$ in equation 32, which leads to $\Delta\mathbf{N}(\mathbf{n}) = 0$ in 31. For $\bar{x} = 1$, we thus have $\mathbf{N} \parallel \mathbf{n}$. In contrast to the P-wave case in the Limestone model, the large deviations extend to larger offsets, decreasing only slowly. This indicates that the SV-wave relative traveltimes errors may extend to larger offsets than in the P-wave case. This is confirmed by comparing Figures 3d and 1d.

In Figure 3d, where we compare the efficiency of various SV-wave moveout formulae, we can see that in the rational approximation 51 (black), the relative traveltimes errors reach nearly 3% for $\bar{x} \sim 1$. All approximations based on the perturbation theory, proposed in this paper, however, have relative traveltimes errors of less than 1%. As expected, the "worst" results are obtained from equation 41 (red), which ignores the difference in directions of \mathbf{N} and \mathbf{n} . It has a maximum error of nearly 0.9% and smaller errors extend to longer offsets. Equation 45 (green) has a maximum error of $\sim 0.4\%$, and the second-order formula in equation 47 (blue) an even smaller error, only $\sim 0.2\%$. Both approximations exhibit some errors only around $\bar{x} \sim 1$. For longer offsets, their errors are negligible.

In Figure 4, we show the results for the SV-wave in the Mesaverde mudshale whose anisotropy is about 12%. From the comparison of exact (black) and first-order (red) phase velocities in Figure 4a, we can see that they are nearly identical in this case. Despite stronger anisotropy, the first-order phase velocity formula performs well. The exact phase (red) and ray (black) velocities shown in Figure 4b, however, differ significantly for offsets $\bar{x} > 1$ (the consequence of strong anisotropy). Although the SV-wave anisotropy of the Mesaverde mudshale is less than half of the P-wave anisotropy of the Greenhorn shale model, the deviations of vectors \mathbf{N} and \mathbf{n} reach nearly the same values, specifically, 14° . Large deviations extend from small to large offsets except for the region around $\bar{x} = 1$, where the two vectors exchange their positions. This has effects on the traveltimes errors shown in Figure 4d. Note that, as in Figure 3d, the angles between the exact vectors \mathbf{N} and \mathbf{n} and between their first-order approximation nearly coincide.

All curves shown in Figure 4d display larger errors than in Figure 3d. For $\bar{x} \sim 1$, the rational approximation 51 (black) has the maximum relative traveltimes error of 11%! The errors slowly decay with increasing offset. The maximum errors of all approximations introduced in this paper are considerably smaller, less than 3%. Formula 41 (red) yields this error for very small offsets. For $\bar{x} \sim 1$ (where vectors \mathbf{N} and \mathbf{n} are parallel), it is around zero and it then again increases to nearly 2% and only slightly decreases with increasing offset. Formulae 45 (green) and 47 (blue) yield nearly identical results in this case, with maximum errors less than 2%.

In Figure 5, we show the results for the SV-wave in the Hard shale model. Its anisotropy is again about 12%. In contrast to the Limestone and Mesaverde mudshale models, the Hard shale model has a large ϵ_W , see Table 1, and thus σ_W , see 30, is positive (it was negative for the two former models). We can see that due to the positive σ_W , the phase-velocity variation with offset in Figure 5a has a different character than in Figures 3a and 4a. Nevertheless, the first-order phase-velocity formula 29 (red) performs relatively well. The variations of the phase (red) and ray (black) velocities are also very similar, see Figure 5b. Figure 5c shows an interesting difference between the first-order

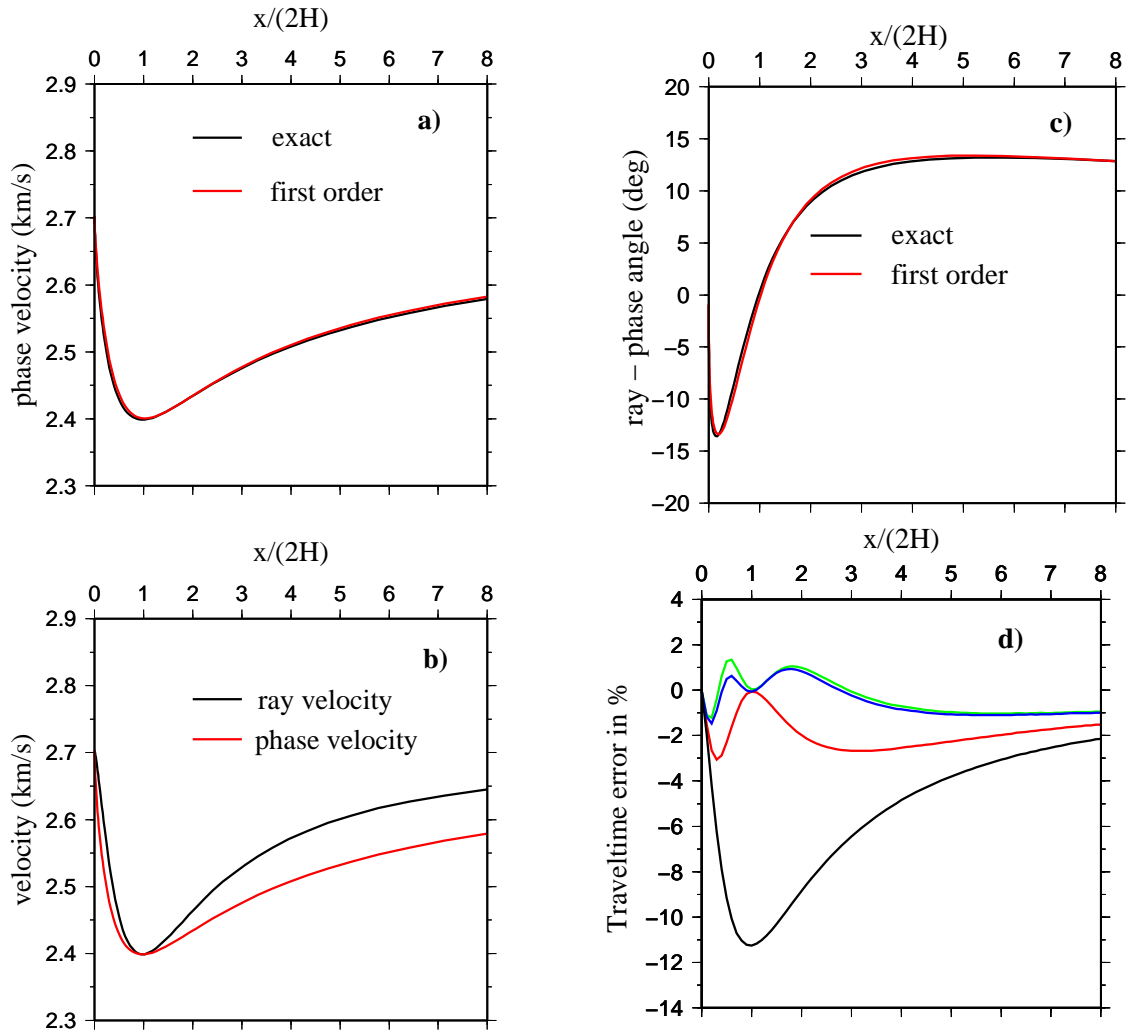


Figure 4: SV-wave moveout in Mesaverde mudshale model, anisotropy $\sim 12\%$. Variation with the normalized offset $\bar{x} = x/2H$ of: a) Exact (black) and first-order (red) phase-velocities. b) Exact ray (black) and phase (red) velocities. c) Angular difference of exact (black) and first-order (red) ray- and phase-velocity directions \mathbf{N} and \mathbf{n} . d) Relative traveltimes errors with traveltimes calculated from the first-order equation 41 ignoring difference in directions of vectors \mathbf{N} and \mathbf{n} - red; from the first-order equation 45 taking into account different directions of \mathbf{N} and \mathbf{n} - green; the second-order equation 47 - blue; the rational approximation 51 - black.

approximation and the exact deviation of vectors \mathbf{N} and \mathbf{n} . The deviation reaches, as in Figure 4c, nearly 14° between $\bar{x} = 0$ and $\bar{x} = 1$. Both the first-order approximation (red) and exact (black) deviations are nearly identical in this interval. For offsets $\bar{x} > 1$, however, the first-order approximation yields much higher values of the deviation, up to

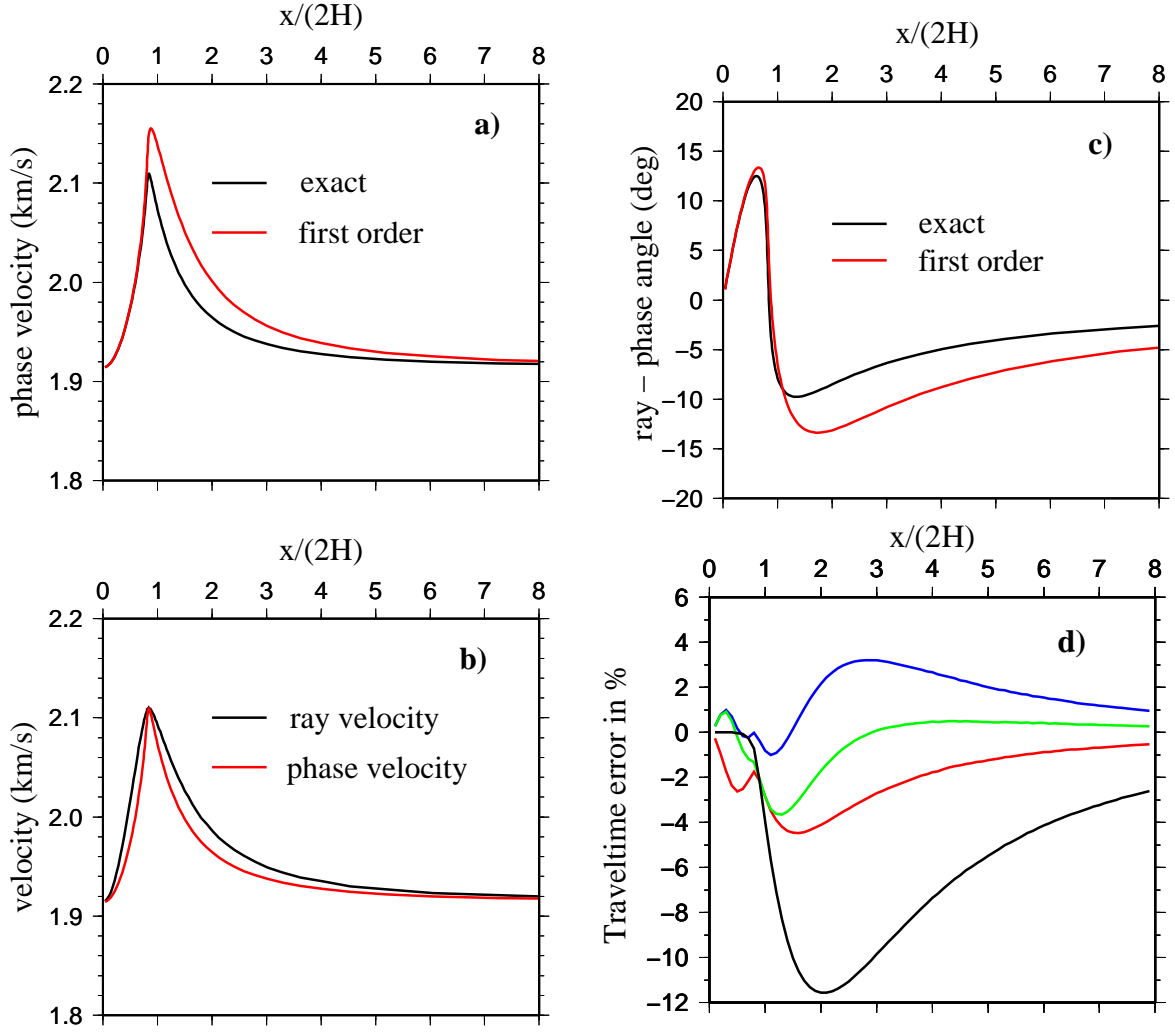


Figure 5: SV-wave moveout in Hard shale model, anisotropy $\sim 12\%$. Variation with the normalized offset $\bar{x} = x/2H$ of: a) Exact (black) and first-order (red) phase-velocities. b) Exact ray (black) and phase (red) velocities. c) Angular difference of exact (black) and first-order (red) ray- and phase-velocity directions \mathbf{N} and \mathbf{n} . d) Relative traveltime errors with traveltime calculated from the first-order equation 41 ignoring difference in directions of vectors \mathbf{N} and \mathbf{n} - red; from the first-order equation 45 taking into account different directions of \mathbf{N} and \mathbf{n} - green; the second-order equation 47 - blue; the rational approximation 51 - black.

14° again, while the maximum exact deviation is less than 10° . This difference is responsible for the large traveltime errors for $\bar{x} > 1$, see Figure 5d.

The comparison of the moveout approximations in Figure 5d shows that rational approximation 51 (black) again has the largest maximum relative traveltime error. For offsets $\bar{x} \sim 2$, it reaches nearly 12%! The maximum errors of the formulae proposed in

this paper are less than 5%. Formula 45 (green) has a maximum error of about 4%, which rapidly decreases for longer offsets. Formula 47 (blue) has a maximum error of about 3%, but it decreases for longer offsets slower than 45. Note, however, that the errors of formula 41 (red) are comparable, and the errors of formulae 45 and 47 are smaller than the errors of the generalized approximation of Stovas (2010), see his Figure 2a.

7 CONCLUSIONS

We propose alternative approximate reflection moveout formulae for P- and SV-waves in homogeneous VTI media. The formulae are based on the weak-anisotropy approximation. They represent expansions with respect to weak-anisotropy parameters. We propose first- and second-order formulae. All depend, at the most, on four parameters: the depth of the single horizontal reflector, vertical velocity and the WA parameters. Some of the formulae depend on an additional parameter, the ratio of the vertical S- and P-wave velocities. This dependence is, however, weak so that a reasonable choice of the ratio affects the accuracy of the moveout formula negligibly.

While the P-wave formulae depend significantly on the separate WA parameters ϵ_W and δ_W , the S-wave formulae depend, most of all, on their difference, $\epsilon_W - \delta_W$. The accuracy of the proposed formulae strongly depends on the difference of directions \mathbf{N} and \mathbf{n} of the ray- and phase-velocity vectors. For offsets, for which the above two vectors are significantly different, the formulae may be less accurate. They become very inaccurate if they ignore this difference as the first-order formula 20 for P-waves and 41 for SV-waves. A great advantage of the proposed formulae is that they all have correct long-offset asymptotes. They, of course, also yield correct values for the zero offset.

As shown by numerical examples, the second-order P-wave formula yields highly accurate results even for strong anisotropy (26%). Stovas' (2010) generalized moveout approximation formula yields even better results, but it is rather complicated when compared with formula 26. The generalized moveout approximation depends on five parameters, while even the second-order formula 26 depends effectively on four parameters only. In case of the SV-wave, the formulae proposed here yield results of comparable or better accuracy than the generalized moveout approximation of Stovas (2010).

The presented formulae are directly applicable to HTI media or media of orthorhombic symmetry. The condition of direct applicability is that the reflector and the ray of the reflected wave are situated in the symmetry planes of the corresponding medium. Generalization of the presented formulae for media, for which the above condition of applicability is not satisfied, for TTI media or media with anisotropy of lower symmetry, and for converted waves is possible. We must only expect more complicated formulae yielding results of lower accuracy. We have already made first attempts to generalize the above moveout formulae for DTI media and for TTI media overlaying a horizontal flat reflector. Under DTI we understand TI media with axes of symmetry perpendicular to dipping plane reflectors (Alkhalifah and Sava, 2010).

Finally, let us mention that, in addition to the moveout formulae, the paper also contains useful formulae relating approximately the ray- and phase-velocity vector directions

in weakly anisotropic media of arbitrary symmetry. Approximate formulae 16, 17 or 37, 38 for the ray velocity squared as a function of the ray incidence angle i may also find useful applications. The normalized offset \bar{x} can be expressed in terms of the angle i as $\bar{x} = 2H \sin i$. It is thus easy to rewrite all the moveout formulae in terms of the ray incidence angle i instead of \bar{x} .

ACKNOWLEDGEMENTS

A substantial part of this work was done during IPs stay at the IPG Paris at the invitation of the IPGP. We are grateful to the Consortium Project "Seismic waves in complex 3-D structures" (SW3D) and the Research Project 210/11/0117 of the Grant Agency of the Czech Republic for support. We are grateful to Claudia Vanelle, Pavel Golikov, Tijmen Jan Moser, Samik Sil, Alexey Stovas and Madhav Vyas for their valuable comments. This paper will appear in the September-October 2013 issue of Geophysics devoted to the proceedings of 15th International Workshop on Seismic Anisotropy.

REFERENCES

- Aleixo, R., and J. Schleicher, 2010, Traveltime approximations for q-P waves in vertical transversely isotropy media: Geophys. Prosp., **58**, 191–201.
- Alkhalifah, T., and P. Sava, 2010, A transversely isotropic medium with a tilted symmetry axis normal to the reflector: Geophysics, **75**, A19A24.
- Alkhalifah, T. and I. Tsvankin, 1995, Velocity analysis for transversely isotropic media: Geophysics, **60**, 1550–1566.
- Backus, G.E., 1965, Possible forms of seismic anisotropy of the uppermost mantle under oceans: J. geophys. Res., **70**, 3429–3439.
- Farra, V., 2001, High order expressions of the phase velocity and polarization of qP and qS waves in anisotropic media: Geophys. J. Int., **147**, 93-105.
- Farra, V., 2004, Improved first-order approximation of group velocities in weakly anisotropic media: Stud. Geophys. Geod., **48**, 199–213.
- Farra, V., and I. Pšenčík, 2003, Properties of the zero-, first- and higher-order approximations of attributes of elastic waves in weakly anisotropic media: J. Acoust. Soc. Am., **114**, 1366–1378.
- Fomel, S., 2004, On anelliptic approximations for qP velocities in VTI media: Geophysical Prospecting, **52**, 247-259.
- Fomel, S., and A. Stovas, 2010, Generalized nonhyperbolic moveout approximation: Geophysics, **75**, U9-U18.
- Fowler, P.J., 2003, Practical VTI approximations: a systematic anatomy: J. Appl. Geophysics, **54**, 347–367.

Gajewski, D., and I. Pšenčík, 1990, Vertical seismic profile synthetics by dynamic ray tracing in laterally varying layered anisotropic structures: *J. Geophys. Res.*, **95**, 11301–11315.

Golikov, P., and A. Stovas, 2012, Accuracy comparison of nonhyperbolic moveout approximations for qP-waves in VTI media: *J. Geophys. Eng.*, **9**, 428–432.

Helbig, K., 1993, Longitudinal directions in media of arbitrary anisotropy: *Geophysics* **58**, 680–691.

Malovichko, A. A., 1978, A new representation of the traveltime curve of reflected waves in horizontally layered media (in Russian): *Applied Geophysics*, **91**, 47-53, English translation in *Sword* (1987).

Pšenčík, I., and V. Farra, 2005, First-order ray tracing for qP waves in inhomogeneous weakly anisotropic media: *Geophysics*, **70**, D65–D75.

Pšenčík, I., and D. Gajewski, 1998, Polarization, phase velocity and NMO velocity of *qP* waves in arbitrary weakly anisotropic media: *Geophysics*, **63**, 1754–1766.

Pšenčík, I., and V. Vavryčuk, 2002, Approximate relation between the ray vector and wave normal directions in weakly anisotropic media: *Stud. geophys. geod.*, **46**, 793-807.

Stovas, A., 2010, Generalized moveout approximation for qP- and qSV-waves in a homogeneous transversely isotropic medium: *Geophysics*, **75**, D79–D84.

Sword, C. H., 1987, A soviet look at datum shift, in *SEP-51: Stanford Exploration Project*, 313-316.

Thomsen, L., 1986, Weak elastic anisotropy: *Geophysics*, **51**, 1954–1966.

Tsvankin, I., 2001, *Seismic signatures and analysis of reflection data in anisotropic media*. Oxford, Elsevier Science Ltd.